Supplementary Information

A facile obtained hypercrosslinked pyrene-based porous organic polymer as high performance electrode materials for lithium-ion batteries

Huiqin Wang,[a] Zhen Li,[b] Zhiying Meng,[b] Xinya Guo,[a] Ya Du*[b] and Haishen Yang*[a]

a. Shanghai Key Laboratory of Materials Protection and Advanced Materials in Electric Power, College of Environmental and Chemical Engineering, Shanghai University of Electric Power, Shanghai 200090, China. E-mail: yanghsh@shiep.edu.cn;

b. Institute of Advanced Synthesis, School of Chemistry and Molecular Engineering, Nanjing Tech University, Nanjing 211816, China. E-mail: ias_ydu@njtech.edu.cn

Materials preparation

Hypercrosslinked pyrene-based porous organic polymer **(HcPPy)** was prepared through a one-step Friedel–Crafts reaction. Pyrene (0.5 g, 2.5 mmol) and dried $CHCl_3$ (16 ml) were sequentially placed in a 100 mL Schlenk tube, under nitrogen atmosphere. After stirred and heated at 60 °C with oil bath for 30 min, $AlCl_3$ (3 g, 22.5 mmol) was slowly added to the reaction flask, and the reaction was heated to 60 °C for 72 h. The reaction was quenched by poured into an ice-water mixture, and the resulting black precipitated product was washed three times with 6 M hydrochloric acid, methyl alcohol, and dichloromethane, respectively. The product was extracted in a Soxhlet extractor with methyl alcohol and dichloromethane for 24 h, respectively. Finally, the obtained black powder was dried in vacuum at 80 °C for 12 h. The produced hypercrosslinked pyrene-based porous organic polymer **(HcPPy)** was yielded (670 mg).

Characterization produced

The Infrared Spectroscopy (IR) of **HcPPy** was obtained from PerkinElmer Spectrum, and the wavenumber from 500 cm^{-1} to 3500 cm^{-1}, The TGA profiles of the **HcPPy** was measured carried out NETZSCH STA 409 PC/PG apparatus with a temperature ramp of 10 °C min^{-1} from 20 °C to 800 °C under a N_2 atmosphere. Nitrogen adsorption–desorption measurements were performed at 77 K using a Quantachrome Autosorb gas-sorption system. Scanning electron microscopes (SEM) was measured on JEOL JSM-7800F. Powder X-ray diffraction (XRD) was measured with a SMARY APEX Ⅱ (Cu-Kα1 irradiation, λ = 1.540598 Å). The porosity of the polymer was characterized by Micromeritics Instrument's Quantachrome Autosorb-iQ3. The specific surface area of the polymer was calculated from its nitrogen adsorption data at a relative pressure of 0.05 to 0.2 according to the Brunauer-Emmet-Teller equation. The pore volume was calculated based on the nitrogen adsorption curve for nitrogen adsorption data at a relative pressure of 0.999. ^{13}C NMR solid-state characterization of **HcPPy** was performed on Agilent 600 M at a spin rate of 8000 kHz. The bulk electronic conductivity of **HcPPy** was measured by the four-point probe ST2742B technology.

Electrochemical measurements

The 2016-coin type cells were used for electrochemical measurements to conduct the charge and discharge performance of the **HcPPy**. The cathode and anode working electrodes were prepared by mixing **HcPPy**: Acetylene black: PVDF (2.5%) with 5:3:2 (weight ratio). After ball milling for two hours, the prepared slurries were

evenly pasted on aluminum foil and Copper foil, respectively. The obtained working electrodes were dried at 80 °C for 12 h in vacuum to remove NMP. The dried working electrodes were cut into discs (14 mm in diameter), and the loading mass of anode electrodes and cathode electrodes were approximately 0.6 and 0.5 mg, respectively. The battery composed of the working electrode, microporous polypropylene film (Celgard 2400) as the separator, nickel foam and stainless steel positive and negative shell and metallic lithium as the reference electrode. 1 M $LiPF_6$ is dissolved in EC/DMC (V:V = 1:1) to prepare the cathode electrode electrolyte. 1 M $LiPF_6$ solution of ethylene carbonate (EC)/dimethyl carbonate (DMC)/ethyl methyl carbonate (EMC) (V:V:V = 1:1:1) was used as the anode electrolyte, respectively. The battery was assembled in a glove box (H_2O<0.01ppm, O_2<0.01ppm). The batteries have an equilibration period for 24 hours before testing, so that the electrolyte is uniformly distributed in the cells. The electrochemical cycle test of the battery was obtained using Neware battery test system (China Neware Technology Co. Ltd.) in a range of 1.5-4.5 V vs. Li^+/Li (cathode) and a range of 0.005-3 V vs. Li^+/Li (anode). Cyclic voltammetry (CV) and electrochemical impedance spectroscopy (EIS) measurements were both instructed on a CHI 760E electrochemical workstation (Shanghai Putian) using the coin cells. For EIS tests, with the voltage amplitude was 5 mV, and the frequency ranging from 10 kHz to 10 MHz. All the electrochemical tests were performed at room temperature.

Supporting Figures

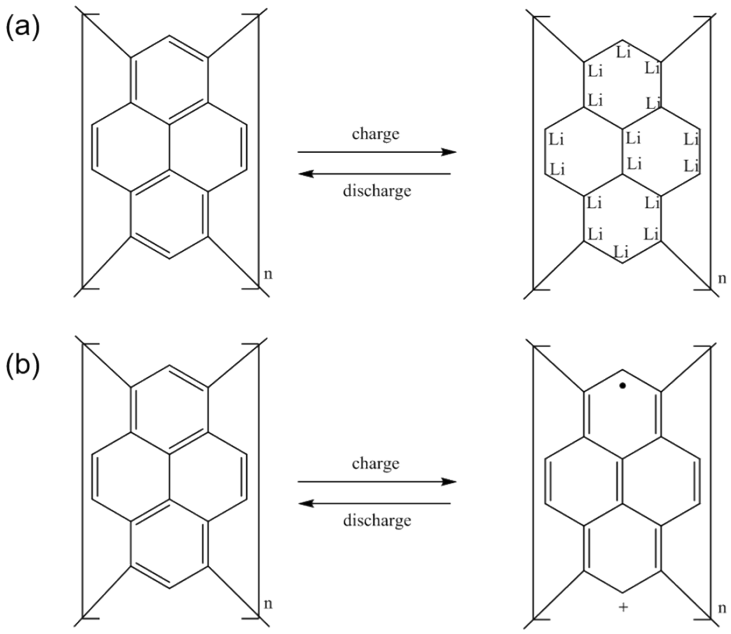

Fig. S1 (a) The reversible charge-discharge process of **HcPPy** as anode; (b) The reversible charge-discharge process of **HcPPy** as cathode.

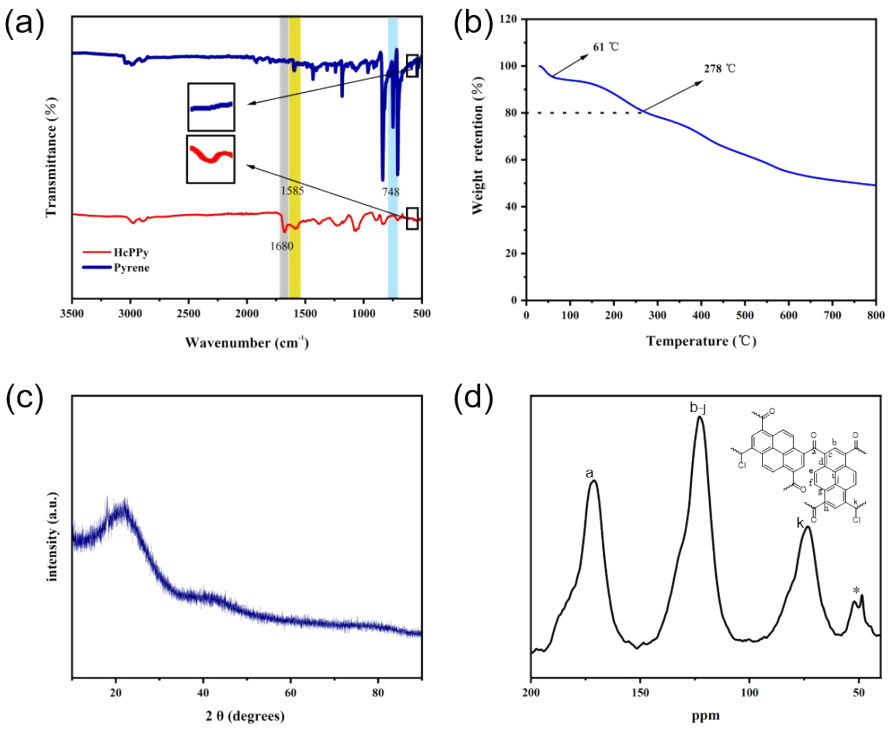

Fig. S2 (a) FTIR spectrum of **HcPPy**; (b) Thermogravimetric analysis (TGA) of **HcPPy**; (c) XRD pattern of **HcPPy**; (d) ^{13}C CP/MAS solid state NMR spectrum.

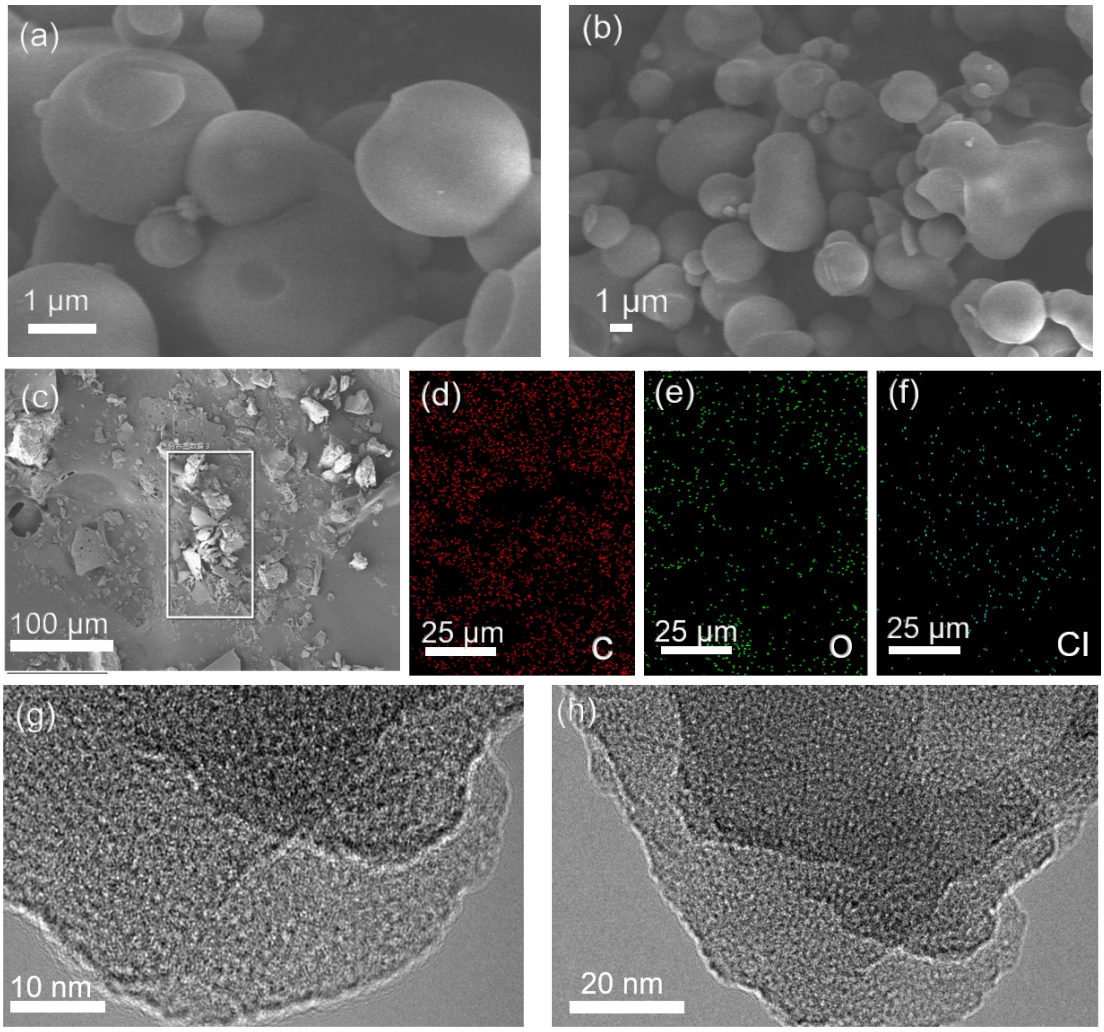

Fig. S3 (a-b) SEM images of **HcPPy**; (c-f) The C, O, Cl element mappings of **HcPPy**; (g-h) HR-TEM images of **HcPPy**.

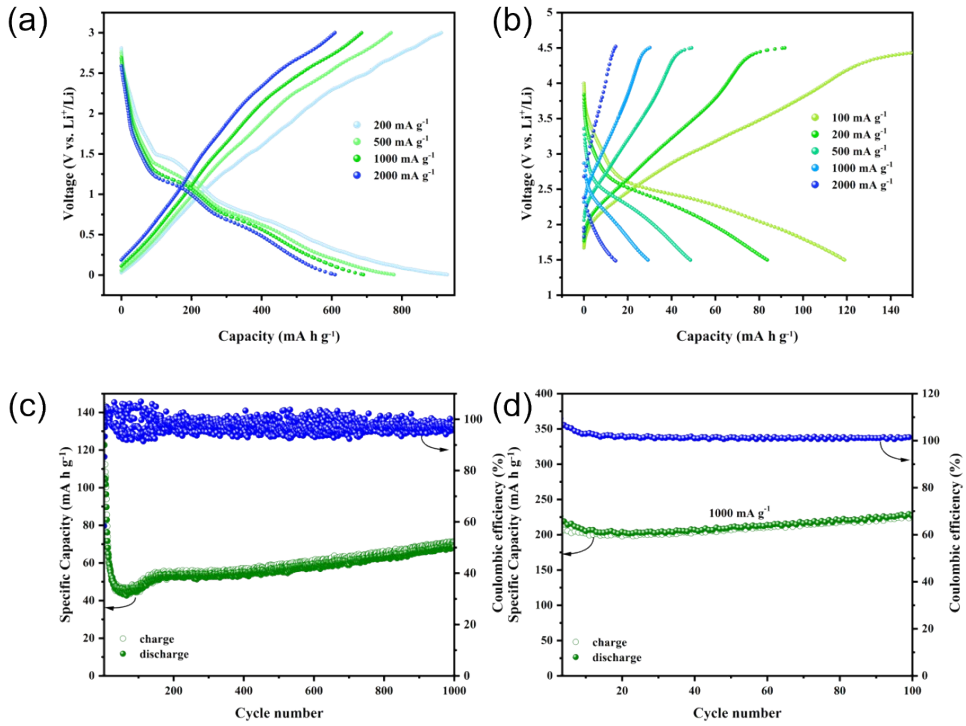

Fig. S4 (a) Charge-discharge curves at different current densities (anode); (b) Charge-discharge curves at different current densities (cathode); (c) Cycling property and coulombic efficiency of **HcPPy** as the cathode at 500 mA g^{-1} with 1000 cycles; (d) Cycling property and coulombic efficiency of acetylene black (AB) without **HcPPy** in the range of 0.005-3.0 V vs. Li^+/Li and at a current density of 1000 mA g^{-1} (AB/PVDF (2.5%) = 7:3).

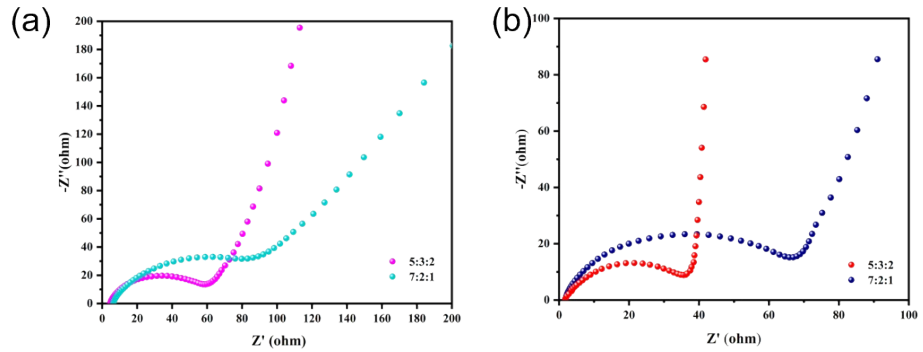

Fig. S5 (a) Electrochemical impedance spectra (EIS) for **HcPPy** as anode; (b) Electrochemical impedance spectra (EIS) for **HcPPy** as cathode.

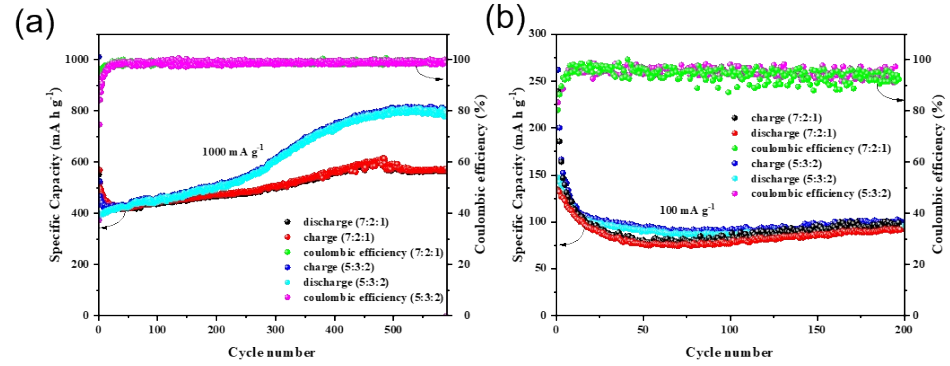

Fig. S6 Experiments with ratio of 7:2:1 and 5:3:2 (**HcPPy**: acetylene black: PVDF) (a) Cycling property and coulombic efficiency of **HcPPy** at 1000 mA g^{-1} as anode for LIBs; (b) Cycling property and coulombic efficiency of **HcPPy** at 100 mA g^{-1} as cathode for LIBs.

Comparison of similar organic electrode materials

Table S1. Comparison of similar organic anode materials

Sample	Theoretical capacity [mA h g^{-1}]	1st discharge capacity [mA h g^{-1}], the current density [mA g^{-1}]/C rate	No. of cycles, capacity retention [%]	Application	Refs
COF	1830;	362, 100;	500^{th}, 90%;	Lithium-Ion Batteries	1
COF@CNTs	1830	1032, 100	500^{th}, 98%		
PAT	1450	1250, 1000	400^{th}, 75%	Lithium-Ion Batteries	2
Maleic acid	1500	870, 2310	500^{th}, 98%	Lithium-Ion Batteries	3
TThPP	686	620, 1000	200^{th}, 61%	Lithium-Ion Batteries	4
PDCzBT	1726	790, 200; 160, 20	400^{th}, 38%; 100^{th}, 90%	Lithium-and Sodium-Ion Batteries	5
HcPPy	2120	1012, 1000	590^{th}, 80%	Lithium-Ion Batteries	This work

Table S2. Comparison of similar organic cathode materials

Sample	Theoretical capacity [mA h g^{-1}]	1st discharge capacity [mA h g^{-1}], the current density [mA g^{-1}]/C rate	No. of cycles, capacity retention [%]	Application	Refs
PYT	408;	275, 1 C;	20^{th}, 40%;	Lithium-Ion Batteries	6
PPYT	262	231, 1 C	500^{th}, 83%		
OPr	258	150, 100	100^{th}, 70%	Sodium-Ion Batteries	7
AQ	258;	250, 0.2 C;	20^{th}, 28%;	Lithium-Ion Batteries	8
LCAQ	174;	85, 0.2 C;	20^{th}, 82%;		
PQ	258;	210, 0.2 C;	20^{th}, 105%;		
LCPQ	174;	90, 0.2 C;	20^{th}, 25%;		
PYT	408;	300, 0.2 C;	20^{th}, 25%;		
LCPYT	296;	217, 0.2 C;	20^{th}, 86%;		
MCPYT	283	242, 0.2 C	20^{th}, 47%		
PyDB	133	120, 100	300^{th}, 139%	Lithium-Ion Batteries	9

Pyrene					
Polypyrene	133;	20, 200;	300^{th}, 50%;	Aluminum Batteries	10
Poly(nitropyrene-co-pyrene)	133; 133	160, 200; 210, 200	300^{th}, 44%; 1000^{th}, 43%		
HcPPy	133	157, 100	200^{th}, 83%	Lithium-Ion Batteries	This work

1 Z. Lei, Q. Yang, Y. Xu, S. Guo, W. Sun, H. Liu, L. P. Lv, Y. Zhang and Y. Wang, *Nat. Commun.*, 2018, **9**, 576.

2 H. Kang, H. Liu, C. Li, L. Sun, C. Zhang, H. Gao, J. Yin, B. Yang, Y. You, K. C. Jiang, H. Long and S. Xin, *ACS Appl. Mater. Interfaces*, 2018, **10**, 37023-37030.

3 Y. Wang, Y. Deng, Q. Qu, X. Zheng, J. Zhang, G. Liu, V. S. Battaglia and H. Zheng, *ACS Energy Lett.*, 2017, **2**, 2140-2148.

4 H. Yang, S. Zhang, L. Han, Z. Zhang, Z. Xue, J. Gao, Y. Li, C. Huang, Y. Yi, H. Liu and Y. Li, *ACS Appl. Mater. Interfaces*, 2016, **8**, 5366-5375.

5 S. Zhang, W. Huang, P. Hu, C. Huang, C. Shang, C. Zhang, R. Yang and G. Cui, *J. Mater. Chem. A*, 2015, **3**, 1896-1901.

6 T. Nokami, T. Matsuo, Y. Inatomi, N. Hojo, T. Tsukagoshi, H. Yoshizawa, A. Shimizu, H. Kuramoto, K. Komae, H. Tsuyama and J. Yoshida, *J. Am. Chem. Soc.*, 2012, **134**, 19694-19700.

7 S. C. Han, E. G. Bae, H. Lim and M. Pyo, *J. Power Sources*, 2014, **254**, 73-79.

8 A. Shimizu, H. Kuramoto, Y. Tsujii, T. Nokami, Y. Inatomi, N. Hojo, H. Suzuki and J.-i. Yoshida, *J. Power Sources*, 2014, **260**, 211-217.

9 Q. He, C. Zhang, X. Li, X. Wang, P. Mu and J. Jiang, *Acta Chim. Sinica*, 2018, **76**, 202-208.

10 M. Walter, K. V. Kravchyk, C. Bofer, R. Widmer and M. V. Kovalenko, *Adv. Mater.*, 2018, **30**, e1705644.